THE JOURNAL OF PHYSICAL CHEMISTRY B

ARTICLE

pubs.acs.org/JPCB

Evaluating How Discrete Water Molecules Affect Protein−DNA $\pi-\pi$ and $\pi^+-\pi$ Stacking and T-Shaped Interactions: The Case of Histidine-Adenine Dimers

Fern M. V. Leavens, Cassandra D. M. Churchill, Siyun Wang, and Stacey D. Wetmore*

Department of Chemistry & Biochemistry, University of Lethbridge, 4401 University Drive, Lethbridge, Alberta, Canada, T1K 3M4

Supporting Information

ABSTRACT: Changes in the magnitude of (M06-2X/6-31+G(d,p)) $\pi-\pi$ stacking and T-shaped (nucleobase-edge and amino acid-edge) interactions between (neutral or protonated) histidine (His) and adenine (A) dimers upon microsolvation with up to four discrete water molecules were determined. A variety of histidine−water interactions were considered including conventional (N−H···O, N···H−O, C−H···O) hydrogen bonding and nonconventional (X−H···π (neutral His) or lone-pair···π (protonated His)) contacts. Overall, the effects of discrete His−H_2O interactions on the neutral histidine−adenine $\pi-\pi$ contacts are negligible (<3 kJ mol^{-1} or 15%) regardless of the type of water binding, the number of water molecules bound, or the His−A dimer (stacked or (amino acid- or nucleobase-edge) T-shaped) configuration. This suggests that previously reported gas-phase binding strengths for a variety of neutral amino acid−nucleobase dimers are likely relevant for a wide variety of (microsolvated) environments. In contrast, the presence of water decreases the histidine−adenine $\pi^+-\pi$ interaction by up to 15 kJ mol^{-1} (or 30%) for all water binding modes and orientations, as well as different stacked and T-shaped His^+-A dimers. Regardless of the larger effect of discrete histidine−water interactions on the magnitude of the $\pi^+-\pi$ compared with $\pi-\pi$ interactions, the $\pi^+-\pi$ binding strengths remain substantially larger than the corresponding $\pi-\pi$ contacts. These findings emphasize the distinct nature of $\pi^+-\pi$ and $\pi-\pi$ interactions and suggest that $\pi^+-\pi$ contacts can provide significant stabilization in biological systems relative to $\pi-\pi$ contacts under many different environmental conditions.

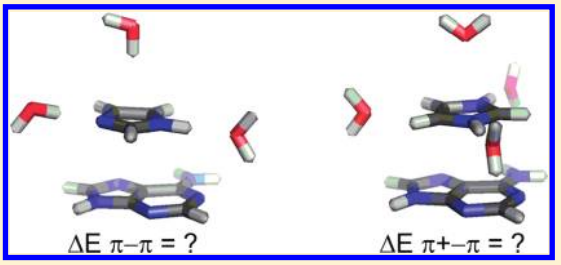

INTRODUCTION

Enzymes responsible for the essential cellular processing of DNA rely on many different noncovalent interactions at the protein−DNA interface.[1] Indeed, noncovalent contacts are used to form the stable, yet readily degradable, protein−DNA complexes required for DNA replication, transcription, and repair.[2,3] For example, repair of DNA damage arising from natural processes (replication errors) or external agents (UV sunlight)[4] uses discrete protein−DNA interactions to selectively identify and remove damaged bases over the natural counterparts.[5−9]

Although the nature of protein−DNA hydrogen-bonding contacts, as well as their importance to cellular function, is well recognized,[10,11] relatively little is known about interactions between the π-systems in biological molecules. Baker and Grant have identified a large number of contacts between the aromatic amino acids in proteins (histidine (His), phenylalanine (Phe), tyrosine (Tyr), and tryptophan (Trp)) and the natural nucleobases in DNA or RNA (adenine (A), cytosine (C), guanine (G), thymine (T), and uracil (U)) in protein−DNA (RNA) complexes.[12] Furthermore, the active sites of a select class of DNA repair enzymes are solely lined with aromatic amino acid residues,[13−15] and therefore protein−DNA $\pi-\pi$ contacts have been proposed to be used to selectively excise detrimental (alkylation) DNA damage.[16,17] Although the exact roles of protein−DNA $\pi-\pi$ interactions have yet to be elucidated, their vast number and types in nature suggest they may be of fundamental importance to life processes.

To better understand the potential impact of protein−DNA $\pi-\pi$ contacts on biological function, our group has used techniques in computational chemistry to evaluate the magnitude of interactions between the aromatic amino acids, including the neutral[18−27] and protonated[25−27] forms of histidine and the natural[19,22−25] or damaged[18,20,21,26,27] DNA/RNA nucleobases. Our approach identifies preferred geometries using detailed potential energy surface scans and evaluates heterodimer interaction energies using the most accurate methods currently possible (CCSD(T)/CBS). Our calculations have provided a detailed comparison of the stacking (face-to-face) and T-shaped (edge-to-face involving an amino acid or nucleobase edge) DNA−protein $\pi-\pi$ interactions.[22,27] This work complements other computational studies that have considered select biomolecules and/or relative monomer orientations.[12,28−33] Collectively, this research shows that protein−DNA stacking and T-shaped $\pi-\pi$ contacts are similar in magnitude to biologically relevant

Received: June 9, 2011
Revised: July 27, 2011
Published: August 02, 2011

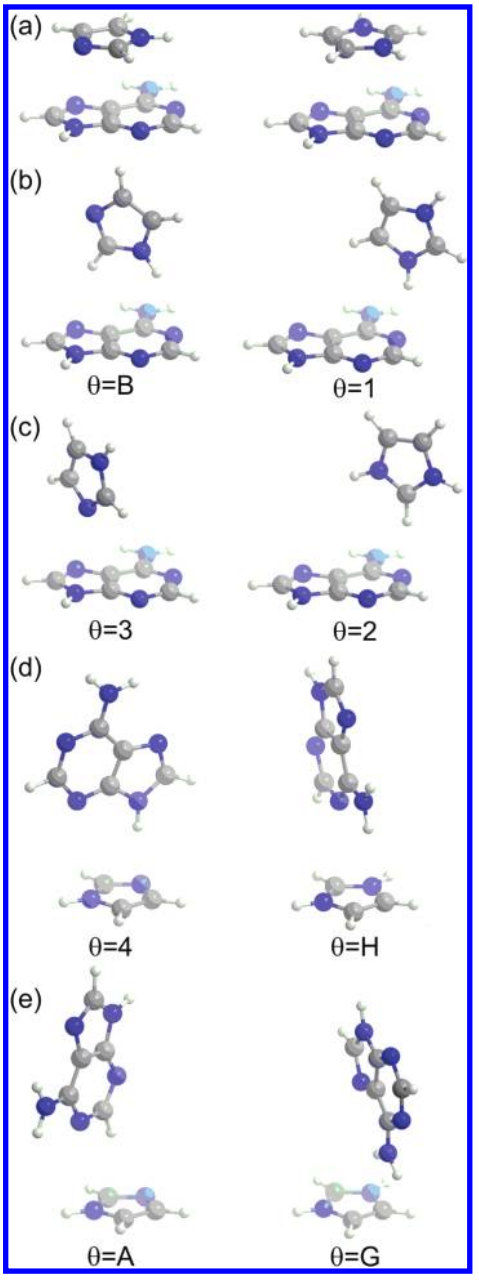

Figure 1. Structure and nomenclature of neutral (left) or protonated (right) histidine−adenine complexes considered in the present work, which include (a) stacked, (b) the strongest, and (c) the weakest amino acid-edge, and the (d) strongest and (e) weakest nucleobase-edge $\pi-\pi$ dimers.

hydrogen-bonding interactions[22] and that $\pi^+-\pi$ interactions (involving protonated histidine or cationic alkylated nucleobases) are even more stable.[18,20,21,25−27,29] Therefore, protein−DNA $\pi-\pi$ and $\pi^+-\pi$ interactions may be an integral part of fundamental biology.

Since previous computational studies of protein−DNA $\pi-\pi$ and $\pi^+-\pi$ interactions primarily used gas-phase calculations,[18−33] predicted binding strengths are specifically relevant to enzyme active sites of low polarity.[34] In attempts to extend applicability to other protein−DNA binding environments, select studies have used implicit solvation methods that rely on a single bulk (dielectric constant) description.[20,29] Unfortunately, it is unclear whether such models accurately portray environmental contributions to the stability of complexes with large intermolecular separations. More importantly, implicit solvation models provide a poor description of the first solvation shell, especially when solute−solvent interactions are strong.[35] Therefore, these models are unlikely to correctly recover changes in $\pi-\pi$ or $\pi^+-\pi$ contacts due to additional discrete interactions, which have been shown to be significant.[36−45] Furthermore, since multiple contacts coexist between residues in protein−DNA complexes,[12] it is expected that implicit solvation models are especially poor approaches for evaluating the strength of noncovalent protein−DNA contacts.

In addition to clarifying how the environment affects the magnitude of $\pi-\pi$ interactions, the relative strength of $\pi-\pi$ and $\pi^+-\pi$ interactions in nature must be assessed in different environments. This is essential for understanding, for example, the extent to which protonation of histidine can stabilize protein−DNA contacts[25] or whether DNA repair enzymes can use $\pi^+-\pi$ interactions to selectively target cationic alkylated nucleobases over natural DNA components.[16−18,20,21,26,27] Although the difference in the magnitude of protein−DNA $\pi-\pi$ and $\pi^+-\pi$ interactions is large in the gas phase,[18,20,21,25−27] $\pi-\pi$ and $\pi^+-\pi$ contacts are distinct classes of noncovalent interactions,[25,26,38,46] and it is not immediately clear how discrete interactions will

Table 1. M06-2X/6-31+G(d,p) Interaction Energies (kJ mol^{-1}) of Neutral Histidine−Adenine Stacked Dimers in the Presence of Discrete Water Molecules[a]

	$\Delta E_{complex}$[b]	ΔE_{His-H_2O}[c]	ΔE_{A-H_2O}[d]	ΔE_{His-A}[e]	$\Delta(\Delta E_{His-A})$[f]
His	−31.8	–	–	−31.8	–
His−HB−a	−41.8	−14.0	3.2	−31.0	−0.8
His−HB−b	−44.4	−14.4	1.6	−31.6	−0.2
His−HB−c	−64.0	−30.9	−0.3	−32.8	1.0
His−HB−d	−74.6	−33.2	−7.4	−34.0	2.2
His−HB−e	−113.5	−67.5	−9.7	−36.3	4.5
His−T	−47.7	−15.8	0.7	−32.6	0.8
	(−47.8)	(−15.6)	(0.0)	(−32.2)	(0.4)
His−HB−a−T	−59.5	−31.9	3.9	−31.5	−0.3
	(−60.2)	(−32.2)	(3.2)	(−31.2)	(−0.6)
His−HB−b−T	−62.0	−32.2	2.3	−32.1	0.3
	(−62.0)	(−31.9)	(1.6)	(−31.7)	(−0.1)
His−HB−c−T	−81.6	−48.9	0.3	−33.0	1.2
	(−82.9)	(−49.9)	(−0.3)	(−32.7)	(0.9)
His−HB−d−T	−87.4	−46.2	−6.8	−34.4	2.6
	(−88.5)	(−46.6)	(−7.4)	(−34.5)	(2.7)
His−HB−e−T	−126.6	−81.5	−9.1	−36.0	4.2
	(−129.6)	(−83.8)	(−9.7)	(−36.1)	(4.3)

[a] See Figure 3 for definition of hydrogen-bonded (HB) and T-shaped (T) histidine−water complexes. For the T-shaped complexes, data with optimal water positions, as well as the water oxygen atom directly above the center of mass of histidine (in parentheses), are reported. [b] $\Delta E_{complex}$ is the interaction energy of the histidine−water−adenine complex. [c] ΔE_{His-H_2O} is the histidine−water interaction energy. [d] ΔE_{A-H_2O} is the sum of the pairwise adenine−water interaction energies. [e] ΔE_{His-A} is the histidine−adenine interaction energy in the solvated complex ($\Delta E_{complex} - \Delta E_{His-H_2O} - \Delta E_{A-H_2O}$). [f] $\Delta(\Delta E_{His-A})$ is the effect of discrete water interactions on the His−A interaction energy, which is calculated as the difference between the interaction energies of the isolated (unsolvated) His−A dimer and the His−A interaction in the histidine−water−adenine complex.

Table 2. M06-2X/6-31+G(d,p) T-Shaped Interaction Energies (kJ mol^{-1}) of Neutral Histidine-Edge Dimers in the Presence of Discrete Water Molecules[a]

edge (θ)		$\Delta E_{complex}$[b]	ΔE_{His-H_2O}[c]	ΔE_{A-H_2O}[d]	ΔE_{His-A}[e]	$\Delta(\Delta E_{His-A})$[f]
B	His	−21.3	–	–	−21.3	–
	His−HB−a	−33.8	−14.0	1.5	−21.3	0.0
	His−HB−d	−58.0	−33.2	−1.4	−23.4	2.1
	His−T	−40.1	−15.8	−1.8	−22.5	1.2
		(−39.4)	(−15.6)	(−1.5)	(−22.3)	(1.0)
	His−HB−a−T	−53.6	−31.4	−0.3	−21.9	0.6
		(−54.0	(−32.0)	(0.0)	(−22.0)	(0.7)
	His−HB−d−T	−79.4	−51.8	−3.2	−24.4	3.1
		(−75.7)	(−48.2)	(−3.0)	(−24.5)	(3.2)
3	His	−12.6	–	–	−12.6	–
	His−HB−a	−27.0	−14.0	0.4	−13.4	0.8
	His−HB−b	−31.7	−14.4	−3.5	−13.8	1.2
	His−HB−c	−44.0	−30.9	0.4	−13.5	0.9
	His−T	−27.1	−15.8	1.9	−13.2	0.6
		(−26.8)	(−15.6)	(1.4)	(−12.6)	(0.0)
	His−HB−a−T	−42.4	−31.6	2.3	−13.1	0.5
		(−43.0)	(−32.0)	(−4.5)	(−6.5)	(−6.1)
	His−HB−b−T	−47.0	−32.0	−1.6	−13.4	0.8
		(−46.9)	(−31.7)	(−2.1)	(−13.1)	(0.5)
	His−HB−c−T	−60.1	−49.2	2.3	−13.2	0.6
		(−61.1)	(−50.0)	(1.8)	(−12.9)	(0.3)

[a] See Figure 3 for definition of hydrogen-bonded (HB) and T-shaped (T) histidine−water complexes and Figure 1 for histidine-edge dimers considered. For the T-shaped complexes, data with optimal water positions, as well as the water oxygen atom directly above the center of mass of histidine (in parentheses), are reported. [b] $\Delta E_{complex}$ is the interaction energy of the histidine−water−adenine complex. [c] ΔE_{His-H_2O} is the histidine−water interaction energy. [d] ΔE_{A-H_2O} is the sum of the pairwise adenine−water interaction energies. [e] ΔE_{His-A} is the histidine−adenine interaction energy in the solvated complex ($\Delta E_{complex} - \Delta E_{His-H_2O} - \Delta E_{A-H_2O}$). [f] $\Delta(\Delta E_{His-A})$ is the effect of discrete water interactions on the His−A interaction energy, which is calculated as difference between the interaction energies of the isolated (unsolvated) His−A dimer and the His−A interaction in the histidine−water−adenine complex.

affect the relative magnitudes of $\pi-\pi$ and $\pi^+-\pi$ binding strengths. Therefore, it is necessary to compare $\pi-\pi$ and $\pi^+-\pi$ interaction energies under different conditions.

The present study complements previous work on protein−DNA stacking and T-shaped interactions between the aromatic amino acids and natural nucleobases by considering the effects of discrete water interactions on the magnitude of $\pi-\pi$ and $\pi^+-\pi$ contacts. Focus is placed on discrete water interactions due to the prevalence of water in biological complexes,[47] where it is often present as a catalytic residue or the product of enzyme catalysis.[47,48] Furthermore, many protein−water and/or DNA−water contacts exist within protein−DNA complexes since water often mediates interactions between the biomolecules[10] or simply fills cavities within a complex.[49] In this light, the effects of microsolvation on the binding strength of heterodimers between neutral (His) or protonated (His$^+$) histidine and adenine (A, Figure 1) will be analyzed by considering discrete contacts between (neutral or protonated) histidine and water. Histidine and adenine dimers were chosen as a case study because of the large number of these contacts in experimental crystal structures,[12] as well as the fact that these are the most widely computationally studied protein−DNA $\pi-\pi$ (and $\pi^+-\pi$) dimers.[18−27,29] Histidine is of particular interest as the point of solvation since it leads to strong $\pi-\pi$ amino acid−nucleobase interactions, which will best allow changes in the binding strength to be observed, and permits investigation of a range of hydrogen-bond acceptor and donor sites,[50−52] and its variable protonation state allows comparison of solvent effects on $\pi-\pi$ versus $\pi^+-\pi$ interactions. For this choice of systems, the most thorough investigation possible was performed, which includes consideration of up to four simultaneous histidine−water interactions, conventional hydrogen bonding,[50,51] less traditional O−H$\cdots\pi$ (neutral His) or lone-pair(O)$\cdots\pi$ (protonated His)[52] histidine−water binding arrangements, and both stacked and T-shaped (amino acid- or nucleobase-edge) histidine−adenine dimers (Figure 1).

Very few studies have investigated the effects of discrete hydrogen-bonding interactions with one or two water molecules on the magnitude of $\pi-\pi$ and $\pi^+-\pi$ stacking interactions between systems that model biologically relevant molecules (amino acids).[36,38] Therefore, the effects of water hydrogen-bonding contacts on ring−ring interactions between biomolecules are not yet well understood. Our work contributes to this area by considering a greater number of (up to four) discrete water contacts, as well as the effects of select O−H$\cdots\pi$ and O$\cdots\pi$ interactions. Furthermore, this is the first time that the effects of discrete solvent (water) interactions on the magnitude of protein−DNA $\pi-\pi$ and $\pi^+-\pi$ contacts are evaluated and compared. Therefore, in addition to contributing to our fundamental knowledge of how discrete contacts with polar molecules affect $\pi-\pi$ and $\pi^+-\pi$ interaction strengths, this study will yield a greater understanding of how the strength of important protein−DNA interactions differs in varying (microsolvated) environments, as well as a better appreciation of the differences between $\pi-\pi$ and $\pi^+-\pi$ interactions in biological systems.

Table 3. M06-2X/6-31+G(d,p) T-Shaped Interaction Energies (kJ mol^{-1}) of Neutral Adenine-Edge (Histidine-Face) Dimers in the Presence of Discrete Water Molecules[a]

edge (θ)		$\Delta E_{complex}$[b]	ΔE_{His-H_2O}[c]	ΔE_{A-H_2O}[d]	ΔE_{His-A}[e]	$\Delta(\Delta E_{His-A})$[f]
4	His	−31.7	–	–	−31.7	–
	His−HB−a	−48.0	−14.0	0.1	−34.1	2.4
	His−HB−b	−48.0	−14.4	−0.3	−33.3	1.6
	His−HB−c	−65.7	−30.9	0.3	−35.1	3.4
	His−HB−d	−65.7	−33.2	0.9	−33.4	1.7
	His−HB−e	−102.7	−67.5	1.0	−36.2	4.5
	His−T	−46.0	−15.8	2.3	−32.5	0.8
		(−45.1)	(−15.6)	(2.0)	(−27.5)	(−4.2)
	His−HB−a−T	−63.2	−31.9	2.4	−33.7	2.0
		(−63.2)	(−32.2)	(2.1)	(−33.1)	(1.4)
	His−HB−b−T	−63.2	−32.2	2.0	−33.0	1.3
		(−62.6)	(−31.9)	(1.7)	(−32.4)	(0.7)
	His−HB−c−T	−81.4	−48.9	2.6	−35.1	3.4
		(−81.9)	(−49.9)	(2.4)	(−34.4)	(2.7)
	His−HB−d−T	−76.3	−52.7	3.1	−26.7	−5.0
		(−76.5)	(−48.7)	(2.9)	(−30.7)	(−1.0)
	His−HB−e−T	−114.9	−88.7	3.3	−29.5	−2.2
		(−116.3)	(−86.0)	(3.0)	(−33.3)	(1.6)
A	His	−9.0	–	–	−9.0	–
	His−HB−a	−22.2	−14.0	1.7	−9.9	0.9
	His−HB−b	−23.4	−14.4	0.5	−9.5	0.5
	His−HB−c	−39.5	−30.9	1.0	−9.6	0.6
	His−HB−d	−43.2	−33.2	−0.2	−9.8	0.8
	His−HB−e	−76.6	−67.5	0.8	−9.9	0.9
	His−T	−25.5	−15.8	−0.1	−9.6	0.6
		(−25.4)	(−15.6)	(−0.3)	(−9.5)	(0.5)
	His−HB−a−T	−39.7	−31.9	1.6	−9.4	0.4
		(−40.4)	(−32.2)	(1.5)	(−9.7)	(0.7)
	His−HB−b−T	−40.9	−32.2	0.4	−9.1	0.1
		(−41.0)	(−31.9)	(0.2)	(−9.3)	(0.3)
	His−HB−c−T	−57.6	−48.9	1.0	−9.7	0.7
		(−58.6)	(−49.9)	(0.8)	(−9.5)	(0.5)
	His−HB−d−T	−62.2	−46.2	−0.3	−15.7	6.7
		(−58.9)	(−46.6)	(−0.4)	(−11.9)	(2.9)
	His−HB−e−T	−97.3	−81.5	0.7	−16.5	7.5
		(−95.1)	(−83.8)	(0.5)	(−11.8)	(2.8)

[a] See Figure 3 for definition of hydrogen-bonded (HB) and T-shaped (T) histidine−water complexes and Figure 1 for adenine-edge dimers considered. For the T-shaped complexes, data with optimal water positions, as well as the water oxygen atom directly above the center of mass of histidine (in parentheses), are reported. [b] $\Delta E_{complex}$ is the interaction energy of the histidine−water−adenine complex. [c] ΔE_{His-H_2O} is the histidine−water interaction energy. [d] ΔE_{A-H_2O} is the sum of the pairwise adenine−water interaction energies. [e] ΔE_{His-A} is the histidine−adenine interaction energy in the solvated complex ($\Delta E_{complex} - \Delta E_{His-H_2O} - \Delta E_{A-H_2O}$). [f] $\Delta(\Delta E_{His-A})$ is the effect of discrete water interactions on the His−A interaction energy, which is calculated as difference between the interaction energies of the isolated (unsolvated) His−A dimer and the His−A interaction in the histidine−water−adenine complex.

COMPUTATIONAL DETAILS

The structures of all monomers and hydrogen-bonded complexes were fully optimized at the MP2/6-31+G(d,p) level of theory. The adenine nucleobase and truncated (neutral and protonated) histidine (modeled as (neutral or protonated) imidazole) were optimized in C_s symmetry, while (neutral and protonated) histidine−water hydrogen-bonded complexes were fully optimized to the relevant point group. The preferred geometries of (neutral and protonated) His−H_2O T-shaped complexes were identified using detailed counterpoise-corrected MP2/6-31+G(d,p) potential energy surface scans analogous to those previously performed in our group[18−27] and outlined in the Supporting Information (SI). From these scans, stable T-shaped complexes with one or two water (O−H) bonds directed toward the (neutral) histidine π-system, as well as the O···π complex between water and protonated histidine, were complexed with adenine. Since water is significantly shifted across the histidine π-system in the most stable relative histidine−water T-shaped orientations, the corresponding His−H_2O T-shaped complexes with water directed at the center of mass of histidine were also

Table 4. M06-2X/6-31+G(d,p) Interaction Energies (kJ mol^{-1}) of Protonated Histidine−Adenine Stacked Dimers in the Presence of Discrete Water Molecules.[a]

	$\Delta E_{complex}$[b]	ΔE_{His-H_2O}[c]	ΔE_{A-H_2O}[d]	ΔE_{His-A}[e]	$\Delta(\Delta E_{His-A})$[f]
His^+	−58.5	–	–	−58.5	–
His^+−HB−a	−99.4	−47.9	2.5	−54.0	−4.5
His^+−HB−b	−110.6	−55.6	−0.2	−54.8	−3.7
His^+−HB−c	−124.1	−75.5	3.7	−52.3	−6.2
His^+−HB−d	−148.3	−99.8	2.2	−50.7	−7.8
His^+−HB−e	−166.7	−118.3	2.0	−50.4	−8.1
His^+−HB−f	−190.5	−145.0	3.5	−49.0	−9.5
His^+−HB−g	−223.9	−183.4	5.6	−46.1	−12.4
His^+−T	−96.5	−41.4	1.3	−56.4	−2.1
	(−96.8)	(−41.6)	(0.6)	(−55.8)	(−2.7)
His^+−HB−a−T	−126.8	−78.0	3.2	−52.0	−6.5
	(−133.0)	(−84.9)	(3.1)	(−51.2)	(−7.3)
His^+−HB−b−T	−142.8	−90.5	0.5	−52.8	−5.7
	(−144.4)	(−92.6)	(0.4)	(−52.2)	(−6.3)
His^+−HB−c−T	−157.2	−111.3	4.5	−50.4	−8.1
	(−157.0)	(−111.4)	(4.3)	(−49.9)	(−8.6)
His^+−HB−d−T	−177.9	−131.8	2.9	−49.0	−9.5
	(−178.8)	(−132.6)	(2.7)	(−48.9)	(−9.6)
His^+−HB−e−T	−197.3	−151.3	2.7	−48.7	−9.8
	(−194.3)	(−148.4)	(2.6)	(−48.5)	(−10.0)
His^+−HB−f−T	−218.9	−175.8	4.2	−47.3	−11.2
	(−218.7)	(−175.8)	(4.0)	(−46.9)	(−11.6)
His^+−HB−g−T	−250.0	−211.5	6.3	−44.8	−13.7
	(−248.6)	(−210.6)	(6.1)	(−44.1)	(−14.4)

[a] See Figure 5 for definition of hydrogen-bonded (HB) and T-shaped (T) histidine−water complexes. For the T-shaped complexes, data with optimal water positions, as well as the water oxygen atom directly above the center of mass of histidine (in parentheses), are reported. [b] $\Delta E_{complex}$ is the interaction energy of the histidine−water−adenine complex. [c] ΔE_{His-H_2O} is the histidine−water interaction energy. [d] ΔE_{A-H_2O} is the sum of the pairwise adenine−water interaction energies. [e] ΔE_{His-A} is the histidine−adenine interaction energy in the solvated complex ($\Delta E_{complex} - \Delta E_{His-H_2O} - \Delta E_{A-H_2O}$). [f] $\Delta(\Delta E_{His-A})$ is the effect of discrete water interactions on the His−A interaction energy, which is calculated as difference between the interaction energies of the isolated (unsolvated) His−A dimer and the His−A interaction in the histidine−water−adenine complex.

bound to adenine (data provided in parentheses in Tables 1−6). Although the shifted and unshifted His−H_2O complexes seldom differ in energy by more than 0.5 kJ mol^{-1}, consideration of both complexes permits evaluation of the impact of the orientation of histidine−water T-shaped contacts on the histidine−adenine binding strengths. The geometries of all His−H_2O T-shaped complexes considered the present study are provided in Figure SI-1 (SI). Complexes with more than one water molecule simultaneously hydrogen-bound and T-shaped to histidine were obtained by overlaying the structure of the preferred (most stable) T-shaped dimer (Figure SI-1, SI) onto a fully optimized histidine−water hydrogen-bonded complex (according to least-squares fitting of the heavy atoms).

In our previous work,[22,25] preferred (neutral and protonated) His−A dimer geometries were identified using MP2/6-31G(d) optimized monomers and MP2/6-31G*(0.25) potential energy surface scans. In the present study, histidine−water−adenine complexes were generated by overlaying MP2/6-31G+(d,p) optimized adenine and His−H_2O complexes onto the preferred His−A dimer geometry previously identified.[22,25] Using the MP2/6-31+G(d,p) rather than MP2/6-31G(d) monomer geometry in MP/6-31G*(0.25) potential energy surface scans do not change the most stable ring−ring orientation or binding energy of isolated (neutral and protonated) His−A dimers (see Tables SI-1−SI-6, SI) and therefore will not alter the histidine−adenine binding strengths reported in the present work. The histidine−adenine complexes that were microsolvated are displayed in Figure 1, where the θ nomenclature used to define the ring edge directed toward the ring face was introduced in our previous publications.[21,22,25] Specifically, the most stable stacked (neutral or protonated) histidine−adenine dimer and amino acid-edge (θ = B (neutral) and 1 (protonated)) and nucleobase-edge (θ = 4 (neutral His) and H (protonated His)) T-shaped dimers were considered. Since the strongest His−H_2O interactions occur with histidine edges that also form the strongest T-shaped interactions with adenine, Histidine−Adenine T-shaped dimers involving other edges were also investigated to elucidate the effects of the strongest histidine−water interactions. Specifically, the amino acid-edge (θ = 3 (neutral) and 2 (protonated)) and nucleobase-edge (θ = A (neutral His) and G (protonated His)) corresponding to the weakest T-shaped dimers were considered. We note that this choice of edges also allows us to compare the effects of discrete water interactions on very strong and very weak T-shaped amino acid−nucleobase dimers. Since previous work did not complete full potential energy surface scans for the weakest T-shaped complexes,[22,25] MP2/6-31G*(0.25)//MP2/6-31G(d) scans were completed for these dimers as per the methodology outlined in our previous publications (see Tables SI-7−SI-10, SI).[18−27]

There is more than one way for nonplanar histidine−water complexes to interact with adenine through stacking or T-shaped interactions, and all combinations were considered in the present work. For example, when a nonplanar His−H_2O hydrogen-bonded complex is stacked with adenine, the water hydrogen atom located out of the histidine molecular plane can directly interact with adenine, or the oxygen lone pair can be directed toward (water hydrogen atom directed away from) adenine. Although each unique arrangement has a different binding strength, the calculated effects of discrete water contacts on the His−A $\pi-\pi$ interaction are very similar. Therefore, due to the abundance of data generated, a representative data set is presented and discussed in the main text, while additional data and figures of different binding arrangements are provided in the Supporting Information (Tables SI-11−SI-16). Specifically, the most stable histidine−water−adenine complexes are considered in the main text when water is hydrogen bound to histidine. When water is T-shaped with respect to histidine, the structures with adenine and water located on the opposite histidine face are reported in the main text for His−A stacked and adenine-edge T-shaped complexes, while water is directed toward N9 of adenine in the reported histidine-edge T-shaped complexes. The same orientations chosen for the individual hydrogen-bonding or T-shaped arrangements are presented for complexes involving both hydrogen-bonding and T-shaped histidine−water interactions for consistency.

Although MP2/6-31G*(0.25) protein−DNA stacking and T-shaped binding strengths are in very good agreement with CCSD(T) values at the complete basis set (CBS) limit,[22,25,27] MP2 has large basis set superposition errors (BSSE),[53] which

Table 5. M06-2X/6-31+G(d,p) T-Shaped Interaction Energies (kJ mol^{-1}) of Protonated Histidine-Edge Dimers in the Presence of Discrete Water Molecules.[a]

edge (θ)		$\Delta E_{complex}$[b]	ΔE_{His-H_2O}[c]	ΔE_{A-H_2O}[d]	ΔE_{His-A}[e]	$\Delta(\Delta E_{His-A})$[f]
1	His^+	−60.7	–	–	−60.7	–
	His^+−HB−a	−103.1	−47.9	1.5	−56.7	−4.0
	His^+−HB−b	−111.0	−55.6	1.6	−57.0	−3.7
	His^+−HB−c	−131.2	−75.5	1.0	−56.7	−4.0
	His^+−HB−d	−150.2	−99.8	3.1	−53.5	−7.2
	His^+−HB−e	−169.1	−118.3	2.5	−53.3	−7.4
	His^+−T	−98.1	−41.4	−0.1	−56.6	−4.1
		(−97.2)	(−41.6)	(0.3)	(−55.9)	(−4.8)
	His^+−HB−a−T	−137.7	−78.0	1.4	−61.1	0.4
		(−136.0)	(−84.9)	(1.8)	(−52.9)	(−7.8)
	His^+−HB−b−T	−142.4	−90.5	1.4	−53.3	−7.4
		(−143.6)	(−92.6)	(1.8)	(−52.8)	(−7.9)
	His^+−HB−c−T	−163.5	−111.3	0.8	−53.0	−7.7
		(−163.0)	(−111.4)	(1.2)	(−52.8)	(−7.9)
	His^+−HB−d−T	−179.2	−131.8	2.9	−50.3	−10.4
		(−179.3)	(−132.6)	(3.3)	(−50.0)	(−10.7)
	His^+−HB−e−T	−198.7	−151.4	2.3	−49.6	−11.1
		(−197.4)	(−149.7)	(2.7)	(−50.4)	(−10.3)
2	His^+	−44.2	–	–	−44.2	–
	His^+−HB−a	−88.8	−47.9	1.0	−41.9	−2.3
	His^+−HB−c	−114.4	−75.5	1.2	−40.1	−4.1
	His^+−HB−e	−154.5	−118.3	2.1	−38.3	−5.9
	His^+−HB−f	−181.2	−145.0	−2.5	−33.7	−10.5
	His^+−HB−g	−217.2	−183.4	−1.8	−32.0	−12.2
	His^+−T	−81.8	−41.4	−8.1	−32.3	−11.9
		(−77.2)	(−41.6)	(−1.4)	(−34.2)	(−10.0)
	His^+−HB−a−T	−131.6	−78.0	−7.2	−46.4	2.2
		(−124.9)	(−84.9)	(−0.4)	(−39.6)	(−4.6)
	His^+−HB−c−T	−155.1	−111.3	−6.9	−36.9	−7.3
		(−149.5)	(−111.4)	(−0.2)	(−37.9)	(−6.3)
	His^+−HB−e−T	−192.5	−149.7	−6.0	−36.8	−7.4
		(−185.6)	(−151.4)	(0.7)	(−34.9)	(−9.3)
	His^+−HB−f−T	−217.0	−175.8	−10.6	−30.6	−13.6
		(−211.1)	(−175.8)	(−3.9)	(−31.4)	(−12.8)
	His^+−HB−g−T	−251.0	−211.5	−10.0	−29.5	−14.7
		(−244.0)	(−210.6)	(−3.2)	(−30.2)	(−14.0)

[a] See Figure 5 for definition of hydrogen-bonded (HB) and T-shaped (T) histidine−water complexes and Figure 1 for protonated histidine-edge dimers considered. For the T-shaped complexes, data with optimal water positions, as well as the water oxygen atom directly above the center of mass of histidine (in parentheses), are reported. [b] $\Delta E_{complex}$ is the interaction energy of the histidine−water−adenine complex. [c] ΔE_{His-H_2O} is the histidine−water interaction energy. [d] ΔE_{A-H_2O} is the sum of the pairwise adenine−water interaction energies. [e] ΔE_{His-A} is the histidine−adenine interaction energy in the solvated complex ($\Delta E_{complex} - \Delta E_{His-H_2O} - \Delta E_{A-H_2O}$). [f] $\Delta(\Delta E_{His-A})$ is the effect of discrete water interactions on the His−A interaction energy, which is calculated as the difference between the interaction energies of the isolated (unsolvated) His−A dimer and the His−A interaction in the histidine−water−adenine complex.

complicates the analysis of discrete interactions in complexes containing different numbers and types of noncovalent interactions.[26] In contrast, the M06-2X functional has small basis set superposition errors for a range of noncovalent interactions.[54] Indeed, protein−DNA $\pi-\pi$ and $\pi^+-\pi$ binding strengths calculated using M06-2X without including BSSE corrections are comparable to CCSD(T)/CBS results.[27] Therefore, the interaction energies reported in the present study were evaluated at the M06-2X/6-31+G(d,p) level of theory (without inclusion of explicit BSSE corrections). We note that that preferred relative monomer orientations identified in the M06-2X/6-31+G(d,p) potential energy surface scans of the isolated His−A dimers are in excellent agreement with those previously identified using MP2/6-31G*(0.25)[22,25] (Tables SI-1−SI-6, SI), which supports the use of the previously reported preferred dimer geometry. Furthermore, the corresponding M06-2X/6-31+G(d,p) binding strengths of isolated His−A dimers are in excellent agreement with previously published MP2/6-31G*(0.25), as well as CCSD(T)/CBS, values[22,25,27] (see Table SI-17, SI).

The total binding energy of each histidine−water−adenine complex was calculated as the difference between the energy of the entire histidine−water−adenine complex ($\Delta E_{complex}$) and

Table 6. M06-2X/6-31+G(d,p) T-Shaped Interaction Energies (kJ mol^{-1}) of Protonated Adenine-Edge (Histidine-Face) Dimers in the Presence of Discrete Water Molecules.[a]

edge (θ)		$\Delta E_{complex}$[b]	ΔE_{His-H_2O}[c]	ΔE_{A-H_2O}[d]	ΔE_{His-A}[e]	$\Delta(\Delta E_{His-A})$[f]
H	His^+	−39.7	–	–	−39.7	–
	His^+−HB−a	−84.3	−47.9	−0.3	−36.1	−3.6
	His^+−HB−b	−91.2	−55.6	0.8	−36.4	−3.3
	His^+−HB−c	−109.5	−75.5	1.1	−35.1	−4.6
	His^+−HB−d	−132.5	−99.8	0.5	−33.2	−6.5
	His^+−HB−e	−150.0	−118.3	0.7	−32.4	−7.3
	His^+−HB−f	−172.9	−145.0	2.1	−30.0	−9.7
	His^+−HB−g	−209.5	−183.4	1.8	−27.9	−11.8
	His^+−T	−77.9	−41.4	1.6	−38.1	−1.6
		(−78.2)	(−41.6)	(1.1)	(−37.7)	(−2.0)
	His^+−HB−a−T	−119.7	−78.0	1.3	−43.0	3.3
		(−118.7)	(−84.9)	(0.9)	(−34.7)	(−5.0)
	His^+−HB−b−T	−123.8	−90.5	2.4	−35.7	−4.0
		(−125.8)	(−92.6)	(1.9)	(−35.1)	(−4.6)
	His^+−HB−c−T	−142.9	−111.3	2.7	−34.3	−5.4
		(−143.0)	(−111.4)	(2.2)	(−33.8)	(−5.9)
	His^+−HB−d−T	−162.2	−131.8	2.2	−32.6	−7.1
		(−163.2)	(−132.6)	(1.7)	(−32.3)	(−7.4)
	His^+−HB−e−T	−180.6	−151.3	2.3	−31.6	−8.1
		(−179.9)	(−148.4)	(1.8)	(−33.3)	(−6.4)
	His^+−HB−f−T	−201.8	−175.8	3.8	−29.8	−9.9
		(−201.9)	(−175.8)	(3.3)	(−29.4)	(−10.3)
	His^+−HB−g−T	−235.9	−211.5	3.4	−27.8	−11.9
		(−235.0)	(−210.6)	(2.9)	(−27.3)	(−12.4)
G	His^+	−1.7	–	–	−1.7	–
	His^+−HB−a	−48.9	−47.9	−1.4	0.4	−2.1
	His^+−HB−b	−56.6	−55.6	0.3	−1.3	−0.4
	His^+−HB−c	−76.3	−75.5	−0.7	−0.1	−1.6
	His^+−HB−d	−99.8	−99.8	−0.9	0.9	−2.6
	His^+−HB−e	−118.8	−118.3	−1.9	1.4	−3.1
	His^+−HB−f	−143.5	−145.0	−1.2	2.7	−4.4
	His^+−HB−g	−182.0	−183.4	−2.5	3.9	−5.6
	His^+−T	−43.2	−41.4	−0.2	−1.6	−0.1
		(−43.3)	(−41.6)	(−0.7)	(−1.0)	(−0.7)
	His^+−HB−a−T	−87.3	−78.0	−1.6	−7.7	6.0
		(−86.4)	(−84.9)	(−2.2)	(0.7)	(−2.4)
	His^+−HB−b−T	−91.7	−90.5	0.1	−1.3	−0.4
		(−94.0)	(−92.6)	(−0.4)	(−1.0)	(−0.7)
	His^+−HB−c−T	−112.6	−111.3	−0.8	−0.5	−1.2
		(−112.6)	(−111.4)	(−1.4)	(0.2)	(−1.9)
	His^+−HB−d−T	−132.0	−131.8	−1.0	0.8	−2.5
		(−133.3)	(−132.6)	(−1.6)	(0.9)	(−2.6)
	His^+−HB−e−T	−152.0	−151.3	−2.1	1.4	−3.1
		(−151.4)	(−148.4)	(−2.6)	(−0.4)	(−1.3)
	His^+−HB−f−T	−175.1	−175.8	−1.4	2.1	−3.8
		(−175.2)	(−175.8)	(−1.9)	(2.5)	(−4.2)
	His^+−HB−g−T	−210.8	−211.5	−2.6	3.3	−5.0
		(−210.1)	(−210.6)	(−3.2)	(3.7)	(−5.4)

[a] See Figure 5 for definition of hydrogen-bonded (HB) and T-shaped (T) histidine−water complexes and Figure 1 for adenine-edge dimers considered. For the T-shaped complexes, data with optimal water positions, as well as the water oxygen atom directly above the center of mass of histidine (in parentheses), are reported. [b] $\Delta E_{complex}$ is the interaction energy of the histidine−water−adenine complex. [c] ΔE_{His-H_2O} is the histidine−water interaction energy. [d] ΔE_{A-H_2O} is the sum of the pairwise adenine−water interaction energies. [e] ΔE_{His-A} is the histidine−adenine interaction energy in the solvated complex ($\Delta E_{complex} - \Delta E_{His-H_2O} - \Delta E_{A-H_2O}$). [f] $\Delta(\Delta E_{His-A})$ is the effect of discrete water interactions on the His−A interaction energy, which is calculated as the difference between the interaction energies of the isolated (unsolvated) His−A dimer and the His−A interaction in the histidine−water−adenine complex.

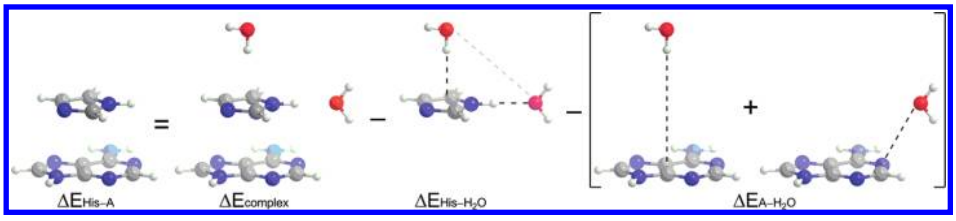

Figure 2. Pictorial representation of the evaluation of the histidine−adenine interaction energy (ΔE_{His-A}) in a microsolvated complex as the difference between the binding strength of the entire histidine−water−adenine complex ($\Delta E_{complex}$), the binding strength of the histidine−water complex (ΔE_{His-H_2O}), which also accounts for water−water interaction energies, and the pairwise adenine−water binding strengths (ΔE_{A-H_2O}).

the sum of the energies of the isolated monomers (A, His, and water(s)) in their individually optimized geometries. To accurately evaluate the His−A $\pi-\pi$ interaction energy in the microsolvated complexes, interactions between water and the histidine or adenine rings, as well as water−water contacts, must be subtracted from $\Delta E_{complex}$. Figure 2 outlines the methodology used in the present work to determine the histidine−adenine binding strength in the microsolvated dimers. Specifically, the total histidine−water interaction energy (ΔE_{His-H_2O}) was determined as the difference in energy between the histidine−water complex and the sum of the energies of the individually optimized histidine and water(s) monomers. Therefore, when ΔE_{His-H_2O} is subtracted from $\Delta E_{complex}$, individual water−water interactions are also removed from the overall complexation energy. To avoid double counting water−water interactions, as well as inaccurately estimating the magnitude of water−water contacts in the solvated complex, the total adenine−water interaction energy (ΔE_{A-H_2O}) was determined as the sum of the interaction energies between adenine and each single water molecule. Thus, the binding strength between histidine and adenine in the explicitly solvated histidine−adenine complex can be calculated by subtracting ΔE_{His-H_2O} and ΔE_{A-H_2O} from the energy of the entire histidine−water−adenine complex ($\Delta E_{complex}$). Since the final histidine−water−adenine complexes were obtained using overlays rather than full optimizations, the reported interaction energies do not include zero-point vibrational energy (ZPVE) corrections.

All calculations were performed with the Gaussian 03[55] and 09[56] program suites.

RESULTS AND DISCUSSION

The present study considers the effects of discrete water molecules interacting with (neutral or protonated) histidine on the magnitude of histidine−adenine stacking and T-shaped $\pi-\pi$ and $\pi^+-\pi$ interactions. In the discussion below, the configurations of stable His−H_2O hydrogen-bonded (denoted by "HB" throughout the manuscript and labeled with a lowercase letter in order of increasing binding strength and number of water molecules bound) and O−H···π or lone-pair(O)···π T-shaped (denoted by "T") complexes will initially be discussed. Subsequently, the effects of discrete His−H_2O interactions on the His−A $\pi-\pi$ binding strengths will be presented for the dimer orientations depicted in Figure 1. It is important to note that the relative orientation of the histidine and adenine rings is set to the arrangement preferred in the isolated (unsolvated) dimer in all complexes regardless of the level of microsolvation. Preliminary calculations indicate that discrete water molecules can significantly affect the preferred ring−ring orientation due to direct interactions between the water molecule(s) and adenine, which is in agreement with observations for other heterodimers.[38] For these dimer geometries, changes in the binding energy relative to the unsolvated dimer result from a complex combination of differences in the histidine−adenine arrangement and discrete intermolecular (solvent) interactions. By maintaining the preferred His−A ring−ring orientation for the isolated (gas-phase) dimer upon solvation, the present work isolates the effects of solvent interactions on the dimer stability. We will first discuss environmental effects on the stability of neutral $\pi-\pi$ histidine−adenine complexes and subsequently those for the corresponding protonated $\pi^+-\pi$ complexes.

Neutral Histidine−Adenine Complexes. *(i) Neutral Histidine−Water Complexes.* Four hydrogen-bonding arrangements between a single water molecule and neutral histidine (imidazole) were identified (Figure 3). Two of the C−H bonds in histidine can act as a proton donor and lead to nearly isoenergetic (stable) minima with nonconventional C−H···O hydrogen-bonding interactions (His−HB−a and His−HB−b). However, the structure containing a single N−H···O interaction (His−HB−c) is more than twice as stable as these complexes. Furthermore, the most stable His−H_2O hydrogen-bonded complex (His−HB−d) contains a single O−H···N interaction. These trends, as well as the calculated magnitude of the binding strengths, are in agreement with results previously published for the (neutral) histidine−water heterodimer.[50,51] Only one complex with more than one water bound to histidine that is void of direct water−water hydrogen-bonding contacts could be isolated in the present work (His−HB−e). As previously noted in the literature,[52] the histidine−water interactions in His−HB−e are synergistic and therefore lead to shorter hydrogen-bond lengths and greater than additive (by 3.4 kJ mol^{-1}) binding energies (ΔE_{His-H_2O}, Table 1). Complexes that involve water−water contacts were not considered in the present work to clearly isolate the effects of discrete histidine−water interactions on $\pi-\pi$ contacts.

In addition to conventional hydrogen-bonding arrangements, complexes containing unconventionial X−H···π interactions can be formed when a small molecule interacts with the π-cloud of histidine.[51] For example, it has been suggested that a quarter of all His residues are involved as acceptors in C−H···π interactions,[57] and unconventional interactions between water and the nitrogen in His residues have also been reported.[58] In the present study, we investigate the stability of O−H···π His−H_2O complexes with one or both water hydrogen atoms directed toward histidine. Although a complex with the water oxygen atom directed at the center of mass of histidine was also considered due to the noted importance of lp···π interactions,[59−61] no minimum could be found using our scanning procedure (see SI for full details). Since the monodentate O−H···π orientation (His−T, Figure 3) is the most stable binding arrangement,[62] only this histidine−water T-shaped complex will be further

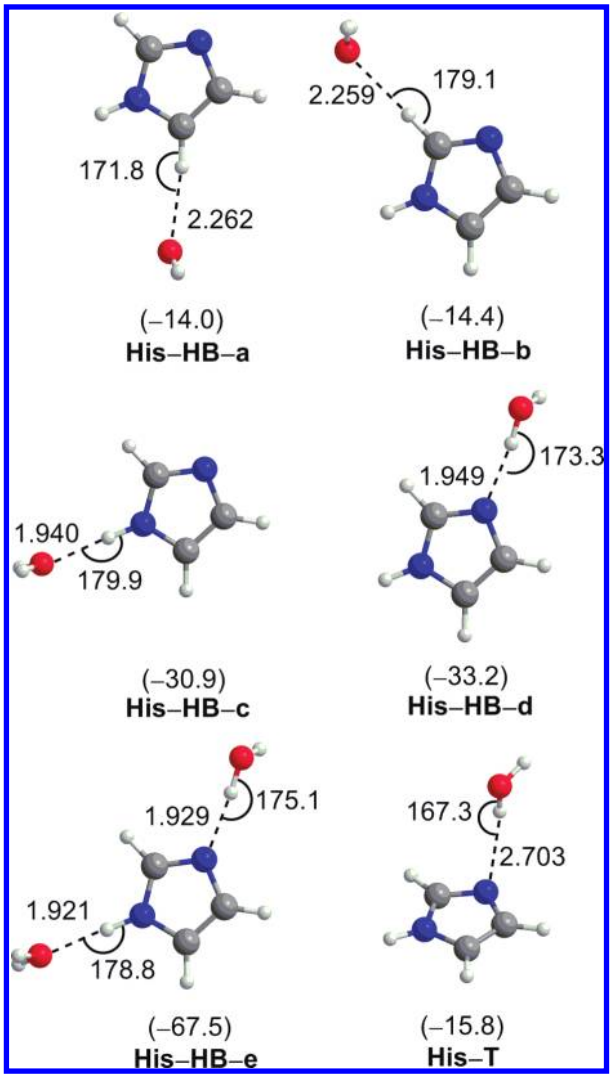

Figure 3. MP2/6-31+G(d,p) hydrogen-bonded (HB) and T-shaped (T) complexes between (neutral) histidine (imidazole) and water. Binding strengths (kJ/mol, in parentheses) obtained from M06-2X/6-31+G(d,p) single-point calculations. Select (MP2/6-31+G(d,p)) hydrogen-bond lengths (Å) and angles (deg) are provided.

discussed. As mentioned in the Computational Details, two T-shaped His−H_2O dimers with this binding orientation were considered: (1) the final structure from our potential energy surface scans with water significantly shifted across the histidine ring (shown in Figure 3), and (2) the complex with water located directly above the histidine center of mass (data provided in parentheses in Tables 1−3). It is interesting to note that combining these optimal T-shaped orientations with the fully optimized hydrogen-bonded complexes leads to additive binding strengths (within 2 kJ mol^{-1}, Table 1). This suggests that the histidine−water T-shaped interactions do not significantly affect the strength of His−H_2O hydrogen-bonding interactions and vice versa. An exception occurs for His−HB−c−T, which exhibits the same (3.4 kJ mol^{-1}) nonadditivity discussed for His−HB−e since both complexes involve a N−H···O interaction and a hydrogen atom directed toward the unprotonated histidine nitrogen (Figure 3).

(ii) Solvation Effects on Neutral Histidine−Adenine Binding Strengths. Figure 4 (left) provides examples of structures of

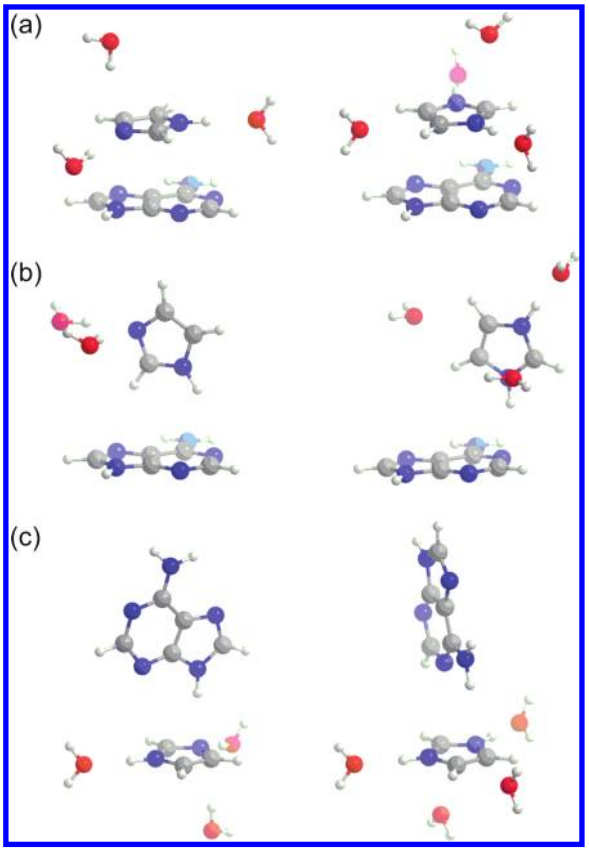

Figure 4. Representative examples of the most highly microsolvated (a) stacked, (b) histidine-edge T-shaped, and (c) nucleobase-edge T-shaped adenine complexes involving neutral (left) or protonated (right) histidine considered in the present work.

microsolvated histidine−adenine stacked and (amino acid or nucleobase) T-shaped dimers considered in the present work. Table 1 outlines the calculated binding strengths ($\Delta E_{complex}$) when various (hydrogen-bonded and T-shaped) histidine−water complexes are stacked with adenine, while Tables 2 and 3 present the corresponding data for histidine-edge and adenine-edge T-shaped interactions, respectively. As discussed in the Computational Details, His−H_2O complexes can bind to adenine in more than one orientation, where representative data are provided in Tables 1−3 and data for the remaining configurations, as well as pictures of the complexes, can be found in the Supporting Information (Tables SI-11−SI-16). Among the results presented in these tables, we are most interested in the magnitude of the histidine−adenine $\pi-\pi$ interaction in the solvated complex (ΔE_{His-A}) and the effects of discrete water interactions on the His−A binding strength ($\Delta(\Delta E_{His-A})$, where a negative number indicates a weaker binding strength upon solvation).

Most neutral dimers strengthen upon microsolvation for all water binding arrangements. This is in agreement with previously reported synergistic effects of, for example, water X−H···π and $\pi-\pi$ stacking interactions[36] or water hydrogen-bonding and T-shaped $\pi-\pi$ interactions.[37] Among the binding arrangements considered, the magnitude of the effects are most significant for the His−HB−d and His−HB−e His−H_2O hydrogen-bonding arrangements (with or without a T-shaped water contact). This is because water is a proton donor and therefore partially

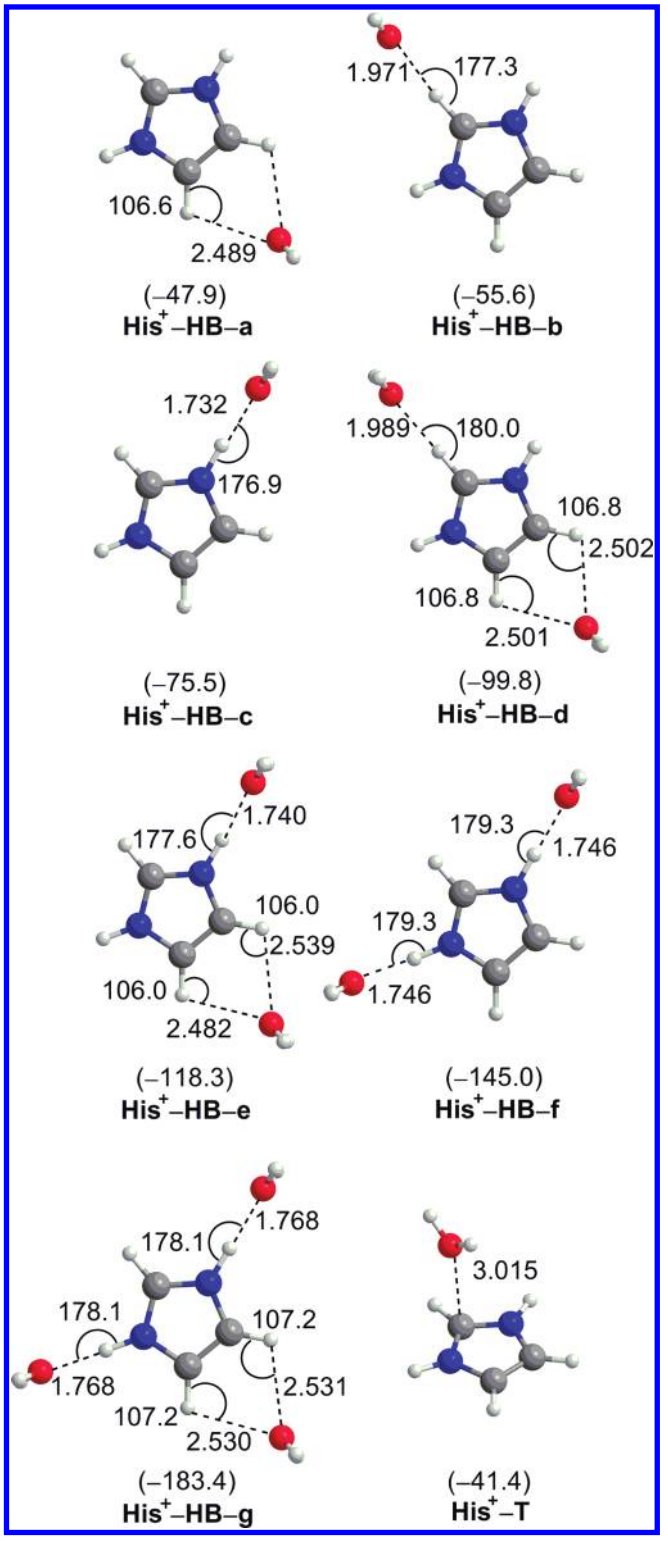

Figure 5. MP2/6-31+G(d,p) hydrogen-bonded (HB) and T-shaped (T) complexes between protonated histidine (imidazole) and water. Binding strengths (kJ/mol, in parentheses) obtained from M06-2X/6-31+G(d,p) single-point calculations and select (MP2/6-31+G(d,p)) hydrogen-bond lengths (Å) and angles (deg) are provided.

protonates the histidine ring in both complexes, which leads to more $\pi^+-\pi$ character. Specifically, the interaction energies of stacked histidine−adenine dimers increase by 3−4 kJ mol^{-1} due

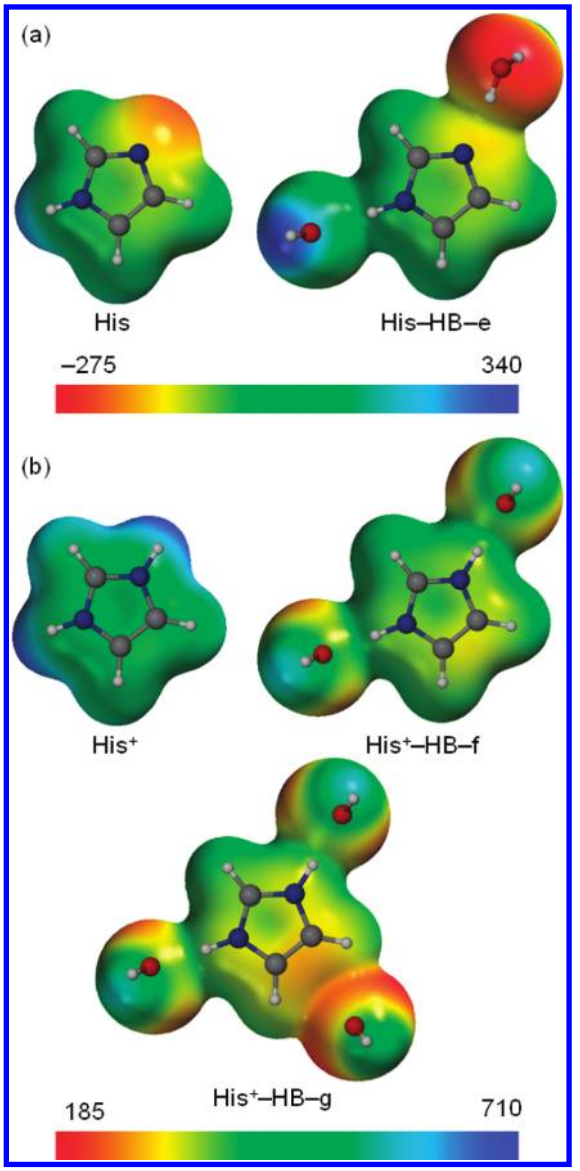

Figure 6. MP2/6-31+G(d) electrostatic potentials (kJ mol^{-1}) of (a) neutral and (b) protonated histidine as well as select histidine−water hydrogen-bonded complexes.

to the greater stability of $\pi^+-\pi$ over $\pi-\pi$ stacking interactions. Similarly, the θ = B histidine-edge T-shaped dimer is (3 kJ mol^{-1}) stronger when a partially charged histidine edge is directed toward electron-rich adenine (Table 2), while the θ = A adenine-edge T-shaped dimer is stabilized (by up to 8 kJ mol^{-1}) when this basic adenine edge is directed toward a more electron-deficient histidine ring (Table 3). In contrast, some His−A interactions weaken due to increased charge on the histidine ring. For example, partial protonation of histidine weakens the θ = 4 adenine-edge T-shaped dimer (by up to 5 kJ mol^{-1}, Table 3) since directing the acidic adenine edge toward histidine is less favorable.

Beyond the interesting trend discussed above for the His−HB−d and His−HB−e His−H_2O binding arrangements, there is no clear correlation between the type or strength of the histidine−water complex and the magnitude of $\Delta(\Delta E_{His-A})$. For example, most His−H_2O hydrogen-bonding interactions increase the strength of the adenine-edge dimers (Table 3),

dx.doi.org/10.1021/jp205424z |J. Phys. Chem. B 2011, 115, 10990–11003

but the magnitudes of the changes do not correlate with the hydrogen-bond donor or acceptor role of histidine. Furthermore, there is no significant difference in the effect of a T-shaped His−H_2O interaction depending on whether a hydrogen atom is directed toward the center of the π-containing histidine ring (in parentheses, Tables 1−3) or is shifted from the center and located above a ring heavy atom (Tables 1−3).

Most importantly, the effects of discrete solvent interactions are small regardless of whether water forms hydrogen bonds or T-shaped interactions with histidine, histidine is the proton donor or acceptor, or the number of water molecules bound. The effects are also small regardless of whether histidine and adenine adopt the most (or least) stable stacked or (amino acid or nucleobase-edge) T-shaped arrangement (Figure 1). Indeed, $\Delta(\Delta E_{His-A})$ is less than 3 kJ mol^{-1} for 85% of all neutral His−A complexes considered, which represents a less than 15% change in the binding strength. It can therefore be concluded that discrete hydrogen-bonding and/or O−H···π T-shaped interactions between up to four water molecules and (neutral) histidine do not significantly affect the strength of histidine−adenine stacking or (amino acid or nucleobase-edge) T-shaped interactions. Thus, the major conclusions drawn in previous (gas-phase) studies[18−33] remain true. Specifically, both stacking and T-shaped protein−DNA π−π interactions are significant in magnitude, where T-shaped interactions are comparable in strength to stacking interactions.[21,22,25] Furthermore, many different T-shaped arrangements (monomer edges) lead to stable π−π dimers even after solvation, where the extremes of the strongest and weakest dimers were considered in the present study.[21,22,25]

The conclusion that discrete histidine−water interactions do not change the magnitude of histidine−adenine π−π interactions can likely be extended to other protein−DNA interactions between two neutral conjugated systems. This finding supports the use of gas-phase calculations to gain information about (neutral) protein−DNA π−π contacts. Specifically, our results suggest that the applicability of previously reported gas-phase binding energies[18−26] can be extended from low polarity (gas-phase) environments[34] to situations where additional (discrete) interactions involve either π-system. This is particularly important when using databases of calculated gas-phase protein−DNA interactions to estimate the strength of π−π contacts observed in experimental crystal structures,[22] where discrete hydrogen-bonding and/or T-shaped interactions with solvent (water)[11,49] or other (R-groups[12] or biological backbone[11,24]) molecules usually also exist.

Protonated Histidine−Adenine Complexes. *(i) Protonated Histidine−Water Complexes.* Upon protonation, histidine loses the ability to act as a hydrogen-bond acceptor. Nevertheless, three hydrogen-bonding arrangements between a single water molecule and protonated histidine (His^+) were identified (Figure 5), which have much stronger binding strengths than the corresponding neutral counterparts (Figure 3). For example, in agreement with previous work,[51] protonation of histidine more than doubles the N−H···O interaction with water (His^+−HB−c) and leads to a five-times stronger C−H···O interaction (His^+−HB−b). A bidentate binding arrangement involving neighboring histidine C−H bonds was also characterized (His^+−HB−a), which has a very large interaction energy (−47.9 kJ mol^{-1}). This structure was not reported in previously published work on interactions between cationic histidine and water since all histidine−water hydrogen bonds were forced to be linear.[51] Due to the variety and strength of the His^+−H_2O hydrogen-bonded complexes, three complexes were optimized that involve two water molecules (His^+−HB−d, e and f) as well as a complex that involves three water molecules (His^+−HB−g), which do not contain discrete water−water contacts.

As discussed for neutral His−H_2O complexes, less conventional T-shaped interactions were also considered between protonated histidine and water. However, the preferred T-shaped orientation directs oxygen toward the π-cloud of cationic histidine (His^+−T, Figure 4), which is similar to other lone-pair···π^+ interactions acknowledged in the literature.[51,59] The lone-pair···π^+ interaction between protonated histidine and water is nearly two and a half times stronger than the O−H···π contact involving neutral histidine. Furthermore, there is not a significant difference in binding strength depending on whether the water oxygen atom is directed toward the center of mass of protonated histidine or shifted across the π-face (ΔE_{His-H_2O}, Table 4).

Unlike discussed for the neutral complexes, the binding strengths are less than the sum of the individual binding strengths by up to 6 kJ mol^{-1} when two water molecules simultaneously hydrogen bond to histidine, which increases to a 15 kJ mol^{-1} deviation from additivity when complexes with three water molecules are considered. When more than one water simultaneously forms T-shaped and hydrogen-bonding interactions with His^+, the binding energies are less than additive by up to 30 kJ mol^{-1}. The deviation from additivity for T-shaped complexes gradually increases from approximately 5−6 kJ mol^{-1} when one N−H···O hydrogen bond is present to 12 kJ mol^{-1} when the weaker C−H···O hydrogen-bonded complex is considered and to 13−17 (29−30) kJ mol^{-1} when two (three) histidine−water hydrogen-bonding interactions occur. Less than additive binding strengths likely occur since partial charge stabilization upon binding of one water decreases the electrostatic contribution to the hydrogen-bonding and/or T-shaped interaction energy for binding of a subsequent water. The large and gradual charge stabilization provided to protonated histidine can be seen in calculated electrostatic potentials (Figure 6), which also illustrate the comparably smaller effect of discrete water contacts on the neutral histidine ring. Thus, the presence of discrete water interactions changes the electrostatic potential of the protonated histidine ring, which will likely also affect the magnitude of π^+−π interactions.

(ii) Solvation Effects on Protonated Histidine−Adenine Binding Strengths. Figure 4 (right) presents representative examples of the microsolvated dimers between protonated histidine and adenine considered in the present work. Tables 4−6 summarize the calculated binding strengths and effects of discrete water molecules on the protonated histidine−adenine π^+−π interaction ($\Delta(\Delta E_{His-A})$) for stacked and (histidine or adenine-edge) T-shaped dimers, respectively. As mentioned for the neutral systems, these data are representative of all possible binding orientations between the His^+−H_2O complexes and adenine, where the corresponding data for other unique binding arrangements are provided in the Supporting Information (Tables SI-11−SI-16). In contrast to the (neutral) His−A dimers, the binding strength between protonated histidine and adenine uniformly decreases upon microsolvation of histidine ($\Delta(\Delta E_{His-A}) < 0$). Furthermore, the effects of discrete water molecules on the π^+−π interaction energies are generally greater than 4 kJ mol^{-1} and therefore are much more significant than those on the neutral His−A π−π dimers. Noteworthy decreases in the binding strength of protonated histidine−phenylalanine (imidazole−benzene) dimers

Table 7. M06-2X/6-31+G(d,p) Histidine−Adenine Interaction Energies in Unsolvated and Microsolvated Protonated Dimers, As Well As the Unsolvated Neutral Dimer with the Same Ring−ring Orientation[a]

His−A dimer[a]	His^+-H_2O complex[b]	His^+−A (unsolvated)[c]	His^+−A (microsolvated)[d]	His−A (unsolvated)[e]
stacking	His^+−HB−g−T	−58.5	−44.8	−21.5
His θ = 1 edge	His^+−HB−e−T	−60.7	−49.6	−22.7
His θ = 2 edge	His^+−HB−g−T	−44.2	−29.5	−6.7
A θ = H edge	His^+−HB−g−T	−39.7	−27.8	−4.4
A θ = G edge	His^+−HB−a−T	−1.7	−7.7	−5.8

[a] See Figure 1 for histidine−adenine dimers considered. [b] See Figure 5 for definition of hydrogen-bonded (HB) and T-shaped (T) histidine−water complexes. [c] Preferred gas-phase His^+−A binding strength. [d] His^+−A binding strength in preferred gas-phase relative ring−ring orientation with the maximum number of water molecules bound to histidine considered in the present study. [e] Gas-phase binding strength between neutral histidine and adenine in the preferred ring−ring orientation of the corresponding protonated histidine dimer.

upon hydrogen bonding water to histidine have been previously reported in the literature.[38]

To better understand the magnitude of the effects of discrete water interactions on $\pi^+-\pi$, we first focus on systematic microsolvation of the His^+−A stacked dimer (Table 4). Hydrogen-bonding interactions between histidine and one water molecule decrease the histidine−adenine stacking interaction by 3.7−6.2 kJ mol^{-1}. Although the range in the effects accounts for different hydrogen-bonding arrangements, there is no direct correlation between the magnitude of the His^+-H_2O hydrogen-bond strength and $\Delta(\Delta E_{His-A})$. A larger reduction in the binding strength occurs with a greater number of water molecules in the complex such that $\Delta(\Delta E_{His-A})$ ranges between 7.8 and 9.5 kJ mol^{-1} when two waters are bound and is 12.4 kJ mol^{-1} when three waters are bound. The decrease in the effect of each additional water in microsolvated His^+−A complexes compared to the effect when only one water is bound is expected based on the nonadditivity of the hydrogen-bonding strengths (discussed above). However, the effects are dampened more than anticipated. Furthermore, when a single water molecule forms a T-shaped interaction with histidine, the His^+−A binding strength decreases by only approximately 2 kJ mol^{-1}, which is a smaller effect than observed for any of the hydrogen-bonded arrangements and is consistent with a weaker His^+-H_2O interaction. Adding a T-shaped His^+-H_2O interaction to any of the (hydrogen-bonded) histidine−water−adenine complexes further decreases the His^+−A stacking energy by approximately 2 kJ mol^{-1}, which suggests the effects of His^+-H_2O T-shaped and hydrogen-bonding contacts are nearly additive.

The general trends discussed for the stacked His^+−A dimer prevail when the strongest histidine-edge (θ = 1, Table 5) and adenine-edge (θ = H, Table 6) T-shaped dimers are considered. $\Delta(\Delta E_{His-A})$ is sometimes greater and sometimes less than those for the corresponding stacked system, and there is no clear trend in the direction of the change. Regardless, $\Delta(\Delta E_{His-A})$ for stacked and T-shaped complexes typically deviates by less than 2 kJ mol^{-1}. Therefore, conclusions drawn in the gas phase regarding the relative stability of stacking and T-shaped dimers[22,25] hold upon microsolvation. Furthermore, the largest effect on the His^+−A interaction energy is 14.4 kJ mol^{-1} regardless of the histidine−adenine dimer type, which represents an up to 30% decrease in the gas-phase $\pi^+-\pi$ interaction energy. In nearly all cases, $\Delta(\Delta E_{His-A}) < 0$ due to a reduction in the net charge on the histidine ring upon hydrogen bonding with water, which can be seen in the electrostatic potentials (Figure 6).

As for neutral histidine, we also considered the protonated histidine (θ = 2, Table 5) and adenine (θ = G, Table 6) edges that lead to weakly stable T-shaped complexes. $\Delta(\Delta E_{His-A})$ for these dimers can be similar to, smaller than, or larger than that for the most stable T-shaped dimer with the same water-binding orientation. However, the percent change in the gas-phase binding energy is consistently larger for the weaker complexes, which leads to two important conclusions. First, the relative stability of different edges previously reported in the gas phase likely remains the same upon microsolvation of the T-shaped dimers. Second, some of the weak T-shaped dimers in the gas phase are even less important in more polar environments. Indeed, the weak θ = G adenine-edge dimer in the gas phase ($\Delta E_{complex}$ = −1.7 kJ mol^{-1}) becomes slightly repulsive when histidine−water hydrogen-bonding interactions are considered (Table 6).

Despite the fact that the decreases in the magnitude of the His^+−A interaction energy upon binding of discrete water molecules to histidine are sizable, the most stable $\pi^+-\pi$ interactions (Table 4−6) are significantly larger than the most stable (neutral) $\pi-\pi$ interactions (Table 1−3) in microsolvated environments. Furthermore, this difference increases more drastically when the same histidine−adenine ring−ring orientations are considered. This is readily seen in Table 7, which compares the binding strength of the isolated (unsolvated) His^+−A dimers, the most highly microsolvated His^+−A dimers considered in the present work, and the (neutral) His−A dimers with the preferred ring−ring orientations of the corresponding protonated systems. Although the effects of up to only four discrete water molecules were considered in the present work, each additional water molecule inflicts a much smaller change in the His^+−A binding strength (Tables 4−6). Therefore, the larger difference between the binding strengths of the discretely solvated protonated dimers (His^+−A (unsolvated)) and neutral dimers (His−A (unsolvated)) compared with the difference between the binding strengths of the unsolvated (His^+−A (unsolvated)) and microsolvated (His^+−A (microsolvated)) protonated histidine dimers (Table 7) suggests that the cationic $\pi^+-\pi$ interactions will be a great deal larger than the corresponding $\pi-\pi$ interactions in even more highly solvated environments.

In summary, unlike $\pi-\pi$ interactions, $\pi^+-\pi$ interactions are affected by additional discrete (water) hydrogen-bonding or T-shaped contacts. Nevertheless, regardless of the level of microsolvation considered in the present work, the $\pi^+-\pi$ interactions are always stronger than the corresponding $\pi-\pi$ interactions. Therefore, the trends in gas-phase protein−DNA $\pi-\pi$ and $\pi^+-\pi$ interactions previously reported[18,20,21,25−27] are valid. Specifically, our data suggest that $\pi^+-\pi$ contacts can provide further stability to biological complexes compared with $\pi-\pi$ contacts in environments where discrete hydrogen-bonding or

T-shaped interactions between solvent (water) or other (R-groups or protein backbone) molecules and the ring systems occur. Differences in the behavior of the $\pi-\pi$ versus $\pi^+-\pi$ interactions upon discrete microsolvation support recent literature suggesting these are two distinct classes of contacts.[25,26,38] Furthermore, the significant difference in the effect of discrete hydrogen-bonding contacts with water on the $\pi^+-\pi$ interactions reported in the present work and the effects on interactions between cationic residues (metal ions) and π-systems previously found[63−66] supports proposals regarding the distinct nature of $\pi^+-\pi$ and cation$-\pi$ interactions.[38]

CONCLUSIONS

The present study closely examines the effects of discrete water (hydrogen-bonding and T-shaped) contacts with histidine on the stability of both neutral and protonated histidine−adenine stacking and (amino acid or nucleobase-edge) T-shaped interactions. Overall, the effects of up to three discrete His$-H_2O$ interactions on the neutral histidine−adenine $\pi-\pi$ contacts are negligible (<3 kJ mol^{-1} or 15%) regardless of the type (N−H···O, N···H−O, C−H···O, or O−H···π) of water binding, the number of water molecules bound, or the His−A dimer (stacked or (amino acid or nucleobase-edge) T-shaped) configuration. Therefore, trends in the previously reported gas-phase binding strengths still hold, which clarify the significant strength of both protein−DNA stacking and T-shaped interactions. It is anticipated that the small effect of microsolvation on the (neutral) histidine−adenine dimer can be extended to other neutral protein−DNA $\pi-\pi$ interactions. These results support the use of gas-phase calculations to gain information about neutral protein−DNA $\pi-\pi$ contacts that appear in a great variety of experimental crystal structures. Specifically, previously published databases of gas-phase amino acid−nucleobase $\pi-\pi$ interaction energies can now confidently be used to analyze contacts occurring in environments of low polarity and environments with select solvent (water) and/or other (R-groups, protein backbone) molecules forming contacts with a neutral π-system.

In contrast to the effect on neutral histidine−adenine interactions, discrete water interactions with protonated histidine more drastically affect the binding strength of protonated histidine−adenine dimers. For all water binding modes and orientations, as well as different stacked and T-shaped His$^+$−A dimers, the presence of water decreases the histidine−adenine $\pi^+-\pi$ interaction (by up to 15 kJ mol^{-1} or 30%). The decrease in the histidine−adenine contact can be rationalized based on at least partial transfer of the positive charge away from the histidine ring, where adenine forms weaker interactions with neutral than protonated histidine. Regardless of the decrease in the His$^+$−A interaction upon binding with water, the (charged) $\pi^+-\pi$ interactions are consistently stronger than the (neutral) $\pi-\pi$ contacts. This supports previous gas-phase findings that $\pi^+-\pi$ interactions provide more significant stabilization to biological complexes compared with (neutral) ring−ring contacts. The unique behavior of discretely solvated $\pi^+-\pi$ and $\pi-\pi$ systems supports recent literature emphasizing the distinct nature of these types of contacts.

ASSOCIATED CONTENT

Supporting Information. Computational details for His$-H_2O$ potential energy surface scans, structures of His$-H_2O$ T-shaped dimers (Figure SI-1), comparison of M06-2X and MP2 preferred geometric variables, and binding strengths of unsolvated histidine−adenine dimers (Tables SI-1−SI-6), complete potential energy surface scans for weak T-shaped dimers (Tables SI-7−SI-10), binding strengths and effects of microsolvation on histidine−adenine complexes with alternate water−adenine relative orientations (Tables SI-11−SI-16), and comparison to CCSD(T)/CBS binding strengths for unsolvated histidine−dimers (Table SI-17). This material is available free of charge via the Internet at http://pubs.acs.org.

AUTHOR INFORMATION

Corresponding Author

*Tel.: +1 403 329 2323. Fax: +1 403 329 2057. E-mail: stacey.wetmore@uleth.ca.

ACKNOWLEDGMENT

We thank the Natural Sciences and Engineering Research Council (NSERC), the Canada Foundation for Innovation (CFI), and the Canada Research Chairs program for financial support. We acknowledge the Upscale and Robust Abacus for Chemistry in Lethbridge (URACIL) for computer resources. F.M.V.L. thanks NSERC for a summer undergraduate research award (USRA). C.D.M.C. thanks NSERC (Julie Payette), Alberta Innovates-Technology Futures, Alberta Scholarship Programs and the University of Lethbridge for student scholarships.

REFERENCES

(1) Voet, D.; Voet, J. G. *Biochemistry*, 3rd ed.; John Wiley & Sons: New York, 2004.
(2) Gromiha, M. M.; Siebers, J. G.; Selvaraj, S.; Kono, H.; Sarai, A. *Gene* **2005**, *364*, 108–113.
(3) Chan, L. L.; Pineda, M.; Heeres, J. T.; Hergenrother, P. J.; Cunningham, B. T. *ACS Chem. Biol.* **2008**, *3*, 437–448.
(4) See, for example: (a) Robertson, K. D.; Jones, P. A. *Carcinogenesis* **2000**, *21*, 461–467. (b) Box, H. C.; Dawidzik, J. B.; Budzinski, E. E. *Free Radical Biol. Med.* **2001**, *31*, 856–868. (c) Gates, K. S. *Chem. Res. Toxicol.* **2009**, *22*, 1747–1760. (d) Kanvah, S.; Joseph, J.; Schuster, G. B.; Barnett, R. N.; Cleveland, C. L.; Landman, U. *Acc. Chem. Res.* **2009**, *43*, 280–287. (e) Cadet, J.; Douki, T.; Ravanat, J.-L. *Free Radical Biol. Med.* **2010**, *49*, 9–21.
(5) Evans, M. D.; Dizdaroglu, M.; Cooke, M. S. *Mutat. Res., Rev. Mutat. Res.* **2004**, *567*, 1–61.
(6) Sedgwick, B.; Bates, P. A.; Paik, J.; Jacobs, S. C.; Lindahl, T. *DNA Repair* **2007**, *6*, 429–442.
(7) Wang, Y. *Chem. Res. Toxicol.* **2008**, *21*, 276–281.
(8) Zharkov, D. O. *Cell. Mol. Life Sci.* **2008**, *65*, 1544–1565.
(9) Robertson, A.; Klungland, A.; Rognes, T.; Leiros, I. *Cell. Mol. Life Sci.* **2009**, *66*, 981–993.
(10) Shrivastav, N.; Li, D.; Essigmann, J. M. *Carcinogenesis* **2010**, *31*, 59–70.
(11) Jones, S.; van Heyningen, P.; Berman, H. M.; Thornton, J. M. J. Mol. Biol. **1999**, *287*, 877–896.
(12) Luscombe, N. M.; Laskowski, R. A.; Thornton, J. M. *Nucleic Acids Res.* **2001**, *29*, 2860–2874.
(13) Baker, C. M.; Grant, G. H. *Biopolymers* **2007**, *85*, 456–470.
(14) Lau, A. Y.; Wyatt, M. D.; Glassner, B. J.; Samson, L. D.; Ellenberger, T. *Proc. Natl. Acad. Sci. U.S.A.* **2000**, *97*, 13573–13578.
(15) Teale, M.; Symersky, J.; DeLucas, L. *Bioconjugate Chem.* **2002**, *13*, 403–407.
(16) Lingaraju, G. M.; Davis, C. A.; Setser, J. W.; Samson, L. D.; Drennan, C. L. *J. Biol. Chem.* **2011**, *286*, 13205–13213.
(17) Stivers, J. T.; Jiang, Y. L. *Chem. Rev.* **2003**, *103*, 2729–2759.

(18) Berti, P. J.; McCann, J. A. B. *Chem. Rev.* **2006**, *106*, 506–555.
(19) Rutledge, L. R.; Campbell-Verduyn, L. S.; Hunter, K. C.; Wetmore, S. D. *J. Phys. Chem. B* **2006**, *110*, 19652–19663.
(20) Rutledge, L. R.; Campbell-Verduyn, L. S.; Wetmore, S. D. *Chem. Phys. Lett.* **2007**, *444*, 167–175.
(21) Rutledge, L. R.; Durst, H. F.; Wetmore, S. D. *Phys. Chem. Chem. Phys.* **2008**, *10*, 2801–2812.
(22) Rutledge, L. R.; Wetmore, S. D. *J. Chem. Theory Comput.* **2008**, *4*, 1768–1780.
(23) Rutledge, L. R.; Durst, H. F.; Wetmore, S. D. *J. Chem. Theory Comput.* **2009**, *5*, 1400–1410.
(24) Churchill, C. D. M.; Navarro-Whyte, L.; Rutledge, L. R.; Wetmore, S. D. *Phys. Chem. Chem. Phys.* **2009**, *11*, 10657–10670.
(25) Churchill, C. D. M.; Rutledge, L. R.; Wetmore, S. D. *Phys. Chem. Chem. Phys.* **2010**, *12*, 14515–14526.
(26) Churchill, C. D. M.; Wetmore, S. D. *J. Phys. Chem. B* **2009**, *113*, 16046–16058.
(27) Rutledge, L. R.; Churchill, C. D. M.; Wetmore, S. D. *J. Phys. Chem. B* **2010**, *114*, 3355–3367.
(28) Rutledge, L. R.; Wetmore, S. D. *Can. J. Chem.* **2010**, *88*, 815–830.
(29) Mao, L.; Wang, Y.; Liu, Y.; Hu, X. *J. Mol. Biol.* **2004**, *336*, 787–807.
(30) Cauet, E.; Rooman, M.; Wintjens, R.; Lievin, J.; Biot, C. *J. Chem. Theory Comput.* **2005**, *1*, 472–483.
(31) Cysewski, P. *Phys. Chem. Chem. Phys.* **2008**, *10*, 2636–2645.
(32) Copeland, K. L.; Anderson, J. A.; Farley, A. R.; Cox, J. R.; Tschumper, G. S. *J. Phys. Chem. B* **2008**, *112*, 14291–14295.
(33) Kee, E. A.; Livengood, M. C.; Carter, E. E.; McKenna, M.; Cafiero, M. *J. Phys. Chem. B* **2009**, *113*, 14810–14815.
(34) Ebrahimi, A.; Habibi-Khorassani, M.; Gholipour, A. R.; Masoodi, H. R. *Theor. Chem. Acc.* **2009**, *124*, 115–122.
(35) Cerny, J.; Hobza, P. *Phys. Chem. Chem. Phys.* **2007**, *9*, 5291–5303.
(36) Marenhich, A. V.; Cramer, C. J.; Truhlar, D. G. *J. Phys. Chem. B* **2009**, *113*, 6378–6396.
(37) Quinonero, D.; Frontera, A.; Escudero, D.; Ballester, P.; Costa, A.; Deya, P. M. *Theor. Chem. Acc.* **2008**, *120*, 385–393.
(38) Escudero, D.; Frontera, A.; Quinonero, D.; Deya, P. M. *J. Phys. Chem. A* **2008**, *112*, 6017–6022.
(39) Singh, N. J.; Min, S. K.; Kim, D. Y.; Kim, K. S. *J. Chem. Theory Comput.* **2009**, *5*, 515–529.
(40) Frontera, A.; Quinonero, D.; Garau, C.; Costa, A.; Ballester, P.; Deya, P. M. *J. Phys. Chem. A* **2006**, *110*, 9307–9309.
(41) Quinonero, D.; Frontera, A.; Garau, C.; Ballester, P.; Costa, A.; Deya, P. M. *ChemPhysChem* **2006**, *7*, 2487–2491.
(42) Frontera, A.; Quinonero, D.; Costa, A.; Ballester, P.; Deya, P. M. *New J. Chem.* **2007**, *31*, 556–560.
(43) Vijay, D.; Zipse, H.; Sastry, G. N. *J. Phys. Chem. B* **2008**, *112*, 8863–8867.
(44) Ebrahimi, A.; Habibi, M.; Neyband, R. S.; Gholipour, A. R. *Phys. Chem. Chem. Phys.* **2009**, *11*, 11424–11431.
(45) Estarellas, C.; Escudero, D.; Frontera, A.; Quinonero, D.; Deya, P. M. *Theor. Chem. Acc.* **2009**, *122*, 325–332.
(46) Vijay, D.; Sastry, G. N. *Chem. Phys. Lett.* **2010**, *485*, 235–242.
(47) Tsuzuki, S.; Mikami, M.; Yamada, S. *J. Am. Chem. Soc.* **2007**, *129*, 8656–8662.
(48) De Beer, S. B. A.; Vermeulen, N. P. E.; Oostenbrink, C. *Curr. Top. Med. Chem.* **2010**, *10*, 55–66.
(49) Ball, P. *Chem. Rev.* **2008**, *108*, 74–104.
(50) Li, Z.; Lazaridis, T. *Phys. Chem. Chem. Phys.* **2007**, *9*, 573–581.
(51) Ornstein, R. L.; Zheng, Y. J. *J. Biomol. Struct. Dyn.* **1997**, *14*, 657–665.
(52) Scheiner, S.; Kar, T.; Pattanayak, J. *J. Am. Chem. Soc.* **2002**, *124*, 13257–13264.
(53) Kar, T.; Scheiner, S. *Int. J. Quantum Chem.* **2006**, *106*, 843–851.
(54) See, for example: (a) Zhao, Y.; Truhlar, D. G. *J. Phys. Chem. A* **2005**, *109*, 6624–6627. (b) Sinnokrot, M. O.; Valeev, E. F.; Sherrill, C. D. *J. Am. Chem. Soc.* **2002**, *124*, 10887–10893. (c) Sponer, J.; Hobza, P. *J. Phys. Chem. A* **2000**, *104*, 4592–4597.
(55) See, for example: (a) Zhao, Y.; Truhlar, D. G. *Theor. Chem. Acc.* **2008**, *120*, 215–241. (b) Zhao, Y.; Truhlar, D. G. *J. Chem. Theory Comput.* **2008**, *4*, 1849–1868.
(56) Frisch, M. J.; Trucks, G. W.; Schlegel, H. B.; Scuseria, G. E.; Robb, M. A.; Cheeseman, J. R.; Montgomery, J., J. A.; Vreven, T.; Kudin, K. N.; Burant, J. C.; et al. *Gaussian 03*, revision D.02; Gaussian, Inc.: Wallingford CT, 2004.
(57) Frisch, M. J.; Trucks, G. W.; Schlegel, H. B.; Scuseria, G. E.; Robb, M. A.; Cheeseman, J. R.; Scalmani, G.; Barone, V.; Mennucci, B.; Petersson, G. A.; et al. *Gaussian 09*, revision A.02; Gaussian, Inc.: Wallingford CT, 2009.
(58) Brandl, M; Weiss, M. S.; Jabs, A.; Sühnel, J.; Hilgenfeld, R. *J. Mol. Biol.* **2001**, *307*, 357–377.
(59) Stoller, E. J.; Gelpí, J. L.; Velankar, S.; Golovin, A.; Orozco, M.; Luisi, B. F. *Proteins* **2004**, *57*, 1–8.
(60) Egli, M.; Sarkhel, S. *Acc. Chem. Res.* **2007**, *40*, 197–205.
(61) Mishra, B. K.; Sathyamurthy, N. *J. Phys. Chem. A* **2007**, *111*, 2139–2147.
(62) Tsuzuki, S.; Mikami, M.; Yamada, S. *J. Am. Chem. Soc.* **2007**, *129*, 8656–8662.
(63) We note that the bidentate arrangement is 1.9 kJ mol^{-1} higher in energy on the MP2/6-31+G(d,p) surface.
(64) Escudero, D.; Frontera, A.; Quinonero, D.; Deya, P. M. *Chem. Phys. Lett.* **2008**, *456*, 257–261.
(65) Estarellas, C.; Frontera, A.; Quinonero, D.; Deya, P. M. *Chem. Phys. Lett.* **2009**, *479*, 316–320.
(66) Rao, J. S.; Zipse, H.; Sastry, G. N. *J. Phys. Chem. B* **2009**, *113*, 7225–7236.
(67) Sharma, B.; Rao, J. S.; Sastry, G. N. *J. Phys. Chem. A* **2011**, *115*, 1971–1984.